

## Supplementary Information

# Atmosphere-Controlled Solvatomorphic Transitions of Ternary Copper(II) Coordination Compounds in Solid State

Darko Vušak, Matea Primožić and Biserka Prugovečki \*

Department of Chemistry, Faculty of Science, University of Zagreb, Horvatovac 102A,  
10000 Zagreb, Croatia; [dvusak@chem.pmf.hr](mailto:dvusak@chem.pmf.hr) (D.V.); [matea.primozic@student.pmf.hr](mailto:matea.primozic@student.pmf.hr) (M.P.)

\* Correspondence: [biserka@chem.pmf.hr](mailto:biserka@chem.pmf.hr)

## 1. Syntheses

**Table S1.** Mechanochemical synthetic conditions and the amounts of reactants and solvents used for the reactions with copper(II) sulfate pentahydrate.

Synthesis number		1	2	3	4	5	6	7
Reactants	$n(\text{CuSO}_4 \cdot 5\text{H}_2\text{O})/\text{mmol}$	0.25	0.25	0.25	0.25	0.25	0.25	0.25
	$m(\text{CuSO}_4 \cdot 5\text{H}_2\text{O})/\text{mg}$	62.3	62.5	62.8	62.1	62.7	62.1	62.3
	$n(\text{Cu}(\text{OH})_2)/\text{mmol}$	0.25	0.25	0.25	0.25	0.25	0.25	0.25
	$m(\text{Cu}(\text{OH})_2)/\text{mg}$	24.8	24.4	24.5	24.6	24.5	24.5	24.5
	$n(\text{bpy})/\text{mmol}$	0.5	0.5	0.5	0.5	0.5	0.5	0.5
	$m(\text{bpy})/\text{mg}$	77.9	78.2	78.4	78.6	78.3	78.1	77.8
	$n(\text{L-ser})/\text{mmol}$	0.5	0.5	0.5	0.5	0.5	0.5	0.5
	$m(\text{L-ser})/\text{mg}$	52.1	52.3	52.3	52.8	52.7	52.5	52.8
Liquid	$\eta/\mu\text{L mg}^{-1}$	-	0.1	0.2	0.1	0.2	0.1	0.2
	$V(\text{H}_2\text{O})/\mu\text{L}$	-	21.7	43.6	10.9	21.8	-	-
	$V(\text{CH}_3\text{OH})/\mu\text{L}$	-	-	-	10.9	21.8	21.7	43.5
Product	<b>1a·6H<sub>2</sub>O + 1a-<math>\alpha</math></b>	<b>1a·6H<sub>2</sub>O</b>	<b>1a·6H<sub>2</sub>O</b>	<b>1a-<math>\alpha</math></b>	<b>1a-<math>\alpha</math></b>	<b>1a-<math>\alpha</math> + UP<sup>a</sup></b>	<b>1a-<math>\alpha</math></b>	
<sup>a</sup> unknown phase(s)								

**Table S2.** Mechanochemical synthetic conditions and the amounts of reactants and solvents used for the reactions with copper(II) sulfate trihydrate and monohydrate.

Synthesis number		8	9	10	11	12	13
Reactants	$n(\text{CuSO}_4 \cdot x\text{H}_2\text{O})/\text{mmol}$	0.25	0.25	0.25	0.25	0.25	0.25
	$m(\text{CuSO}_4 \cdot x\text{H}_2\text{O})/\text{mg}$	53.8	53.6	53.2	44.3	44.3	44.4
	$x$	3	3	3	1	1	1
	$n(\text{Cu}(\text{OH})_2)/\text{mmol}$	0.25	0.25	0.25	0.25	0.25	0.25
	$m(\text{Cu}(\text{OH})_2)/\text{mg}$	24.3	24.6	24.5	24.9	24.9	24.2
	$n(\text{bpy})/\text{mmol}$	0.5	0.5	0.5	0.5	0.5	0.5
	$m(\text{bpy})/\text{mg}$	78.3	78.1	78.0	78.5	78.6	78.1
	$n(\text{L-ser})/\text{mmol}$	0.5	0.5	0.5	0.5	0.5	0.5
	$m(\text{L-ser})/\text{mg}$	52.6	52.7	52.7	52.6	52.0	52.6
Liquid	$\eta/\mu\text{L mg}^{-1}$	0.1	0.2	-	0.1	0.2	-
	$V(\text{CH}_3\text{OH})/\mu\text{L}$	20.9	41.8	-	20.0	40.0	-
	Product	<b>1a-<math>\alpha</math> + UP<sup>a</sup></b>	<b>1a-<math>\alpha</math> + UP<sup>a</sup></b>	- <sup>b</sup>	<b>1a-<math>\alpha</math></b>	<b>1a-<math>\alpha</math></b>	- <sup>c</sup>
<sup>a</sup> unknown phase(s) <sup>b</sup> very small amount of new phases formed, possibly <b>1a-<math>\alpha</math></b> and unknown phases <sup>c</sup> no reaction							

**Table S3.** Mechanochemical synthetic conditions and the amounts of reactants and solvents used for the reactions with anhydrous copper(II) sulfate.

Synthesis number		14	15	16	17	18	19
Reactants	<i>n</i> (CuSO <sub>4</sub> )/mmol	0.25	0.25	0.25	0.25	0.25	0.25
	<i>m</i> (CuSO <sub>4</sub> )/mg	39.6	40.1	39.0	40.2	39.9	39.9
	<i>n</i> (Cu(OH) <sub>2</sub> )/mmol	0.25	0.25	0.25	0.25	0.25	0.25
	<i>m</i> (Cu(OH) <sub>2</sub> )/mg	24.3	24.6	24.3	24.6	24.2	24.2
	<i>n</i> (bpy)/mmol	0.5	0.5	0.5	0.5	0.5	0.5
	<i>m</i> (bpy)/mg	78.0	78.1	78.4	78.1	78.0	78.3
Liquid	<i>n</i> (L-ser)/mmol	0.5	0.5	0.5	0.5	0.5	0.5
	<i>m</i> (L-ser)/mg	52.7	52.7	52.8	52.6	52.3	52.7
Liquid	$\eta/\mu\text{L mg}^{-1}$	-	0.1	0.2	0.4	0.6	1.8
	<i>V</i> (CH <sub>3</sub> OH)/ $\mu\text{L}$	-	19.6	38.9	78.2	116.6	351.2
	Product	- <sup>a</sup>	<b>1a-<math>\alpha</math></b>	<b>1a-<math>\alpha</math></b>	<b>1a-<math>\alpha</math> + UP<sup>b</sup></b>	<b>1a-<math>\alpha</math> + UP<sup>b</sup></b>	<b>1a-<math>\alpha</math><sup>c</sup> + 1b·3CH<sub>3</sub>OH<sup>c</sup></b>
<sup>a</sup> no reaction <sup>b</sup> unknown phase(s) <sup>c</sup> It is possible that <b>1a-<math>\alpha</math></b> does not form in reaction but only after decomposition of <b>1b·3CH<sub>3</sub>OH</b> . PXRD experiment was conducted ex situ.							

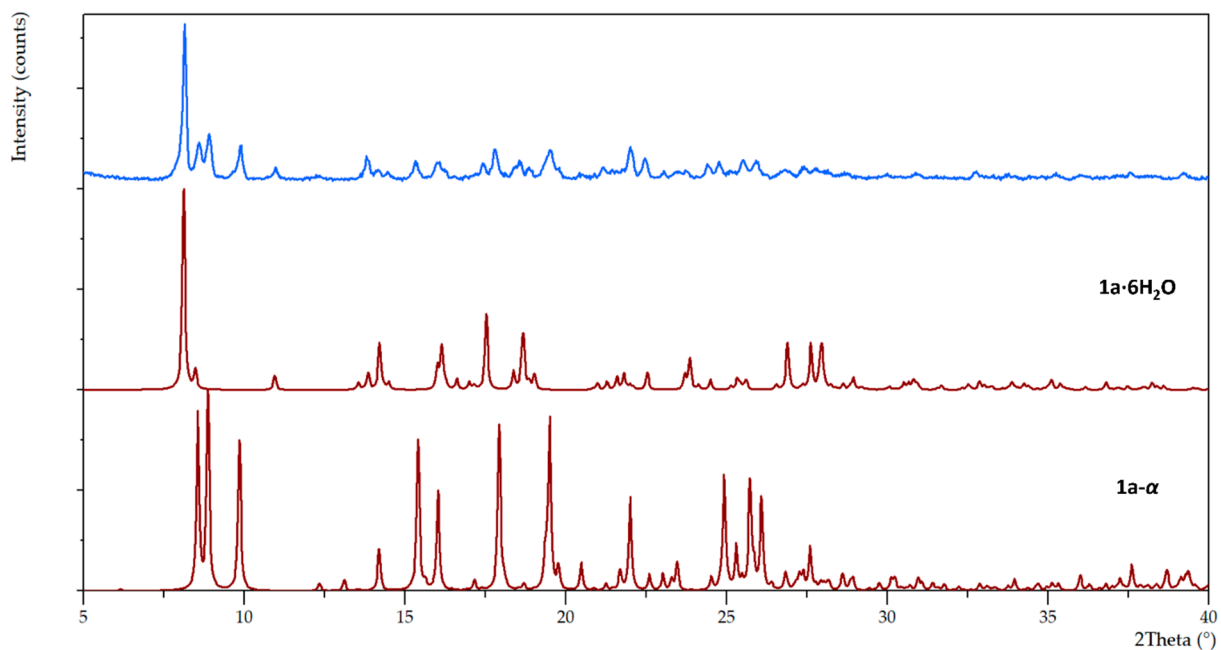


**Figure S1.** Experimental PXRD pattern (blue) of the products of synthesis no. 1 from Table S1 compared with calculated PXRD patterns from the crystal structures of **1a- $\alpha$**  and **1a·6H<sub>2</sub>O** (red).

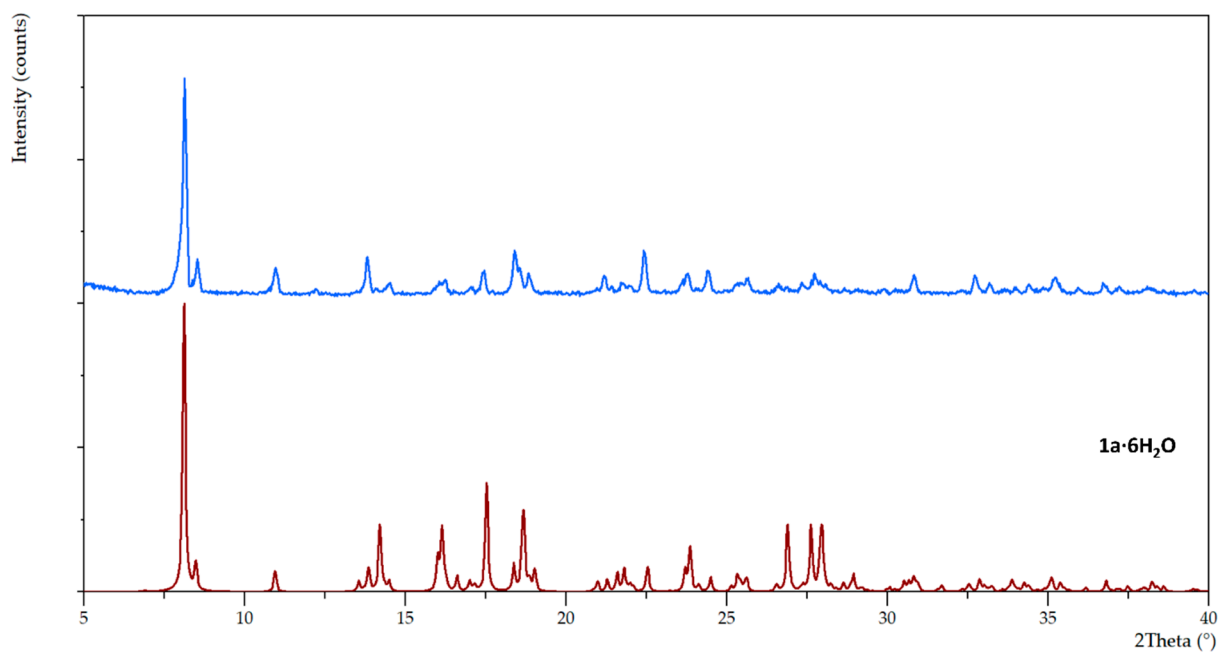


**Figure S2.** Experimental PXRD pattern (blue) of the products of synthesis no. 2 from Table S1 compared with calculated PXRD patterns from the crystal structure of **1a- $\alpha$**  (red).

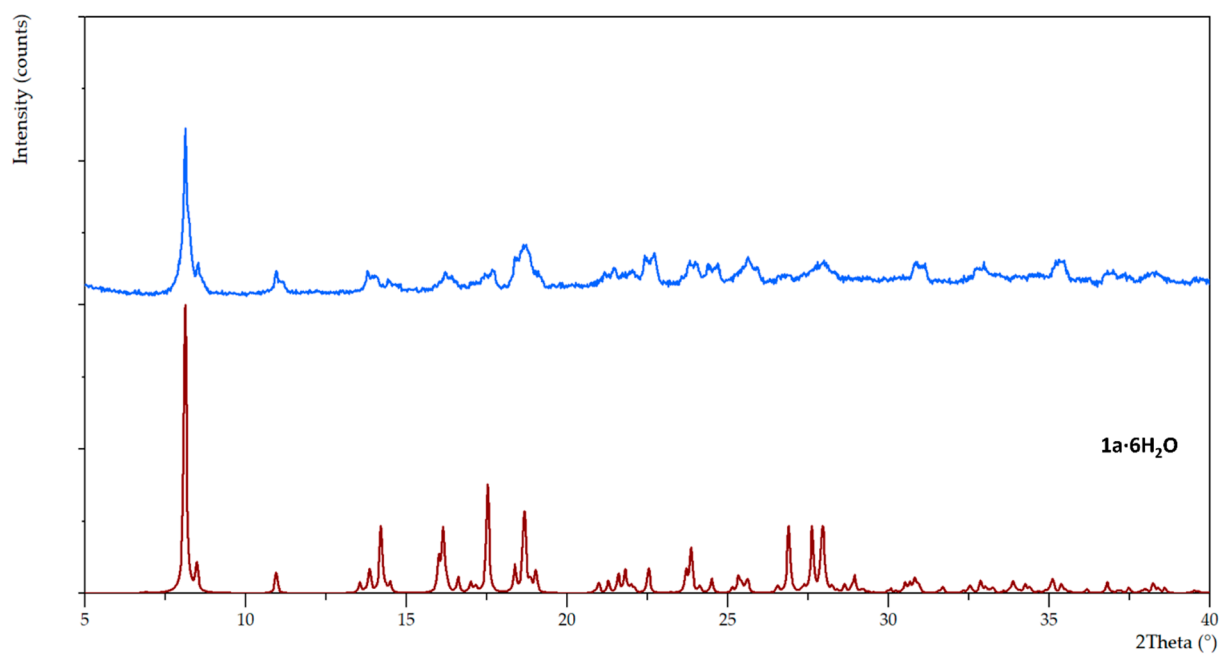


**Figure S3.** Experimental PXRD pattern (blue) of the products of synthesis no. 3 from Table S1 compared with calculated PXRD patterns from the crystal structure of **1a- $\alpha$**  (red).

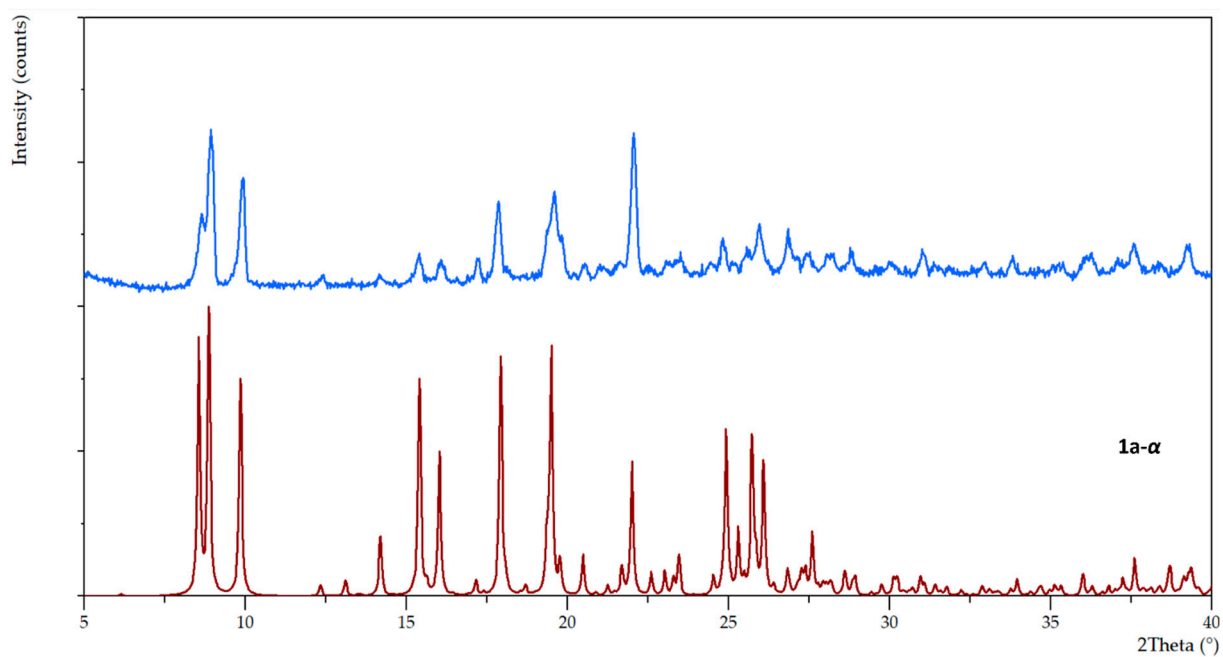


**Figure S4.** Experimental PXRD pattern (blue) of the products of synthesis no. 4 from Table S1 compared with calculated PXRD patterns from the crystal structure of **1a- $\alpha$**  (red).

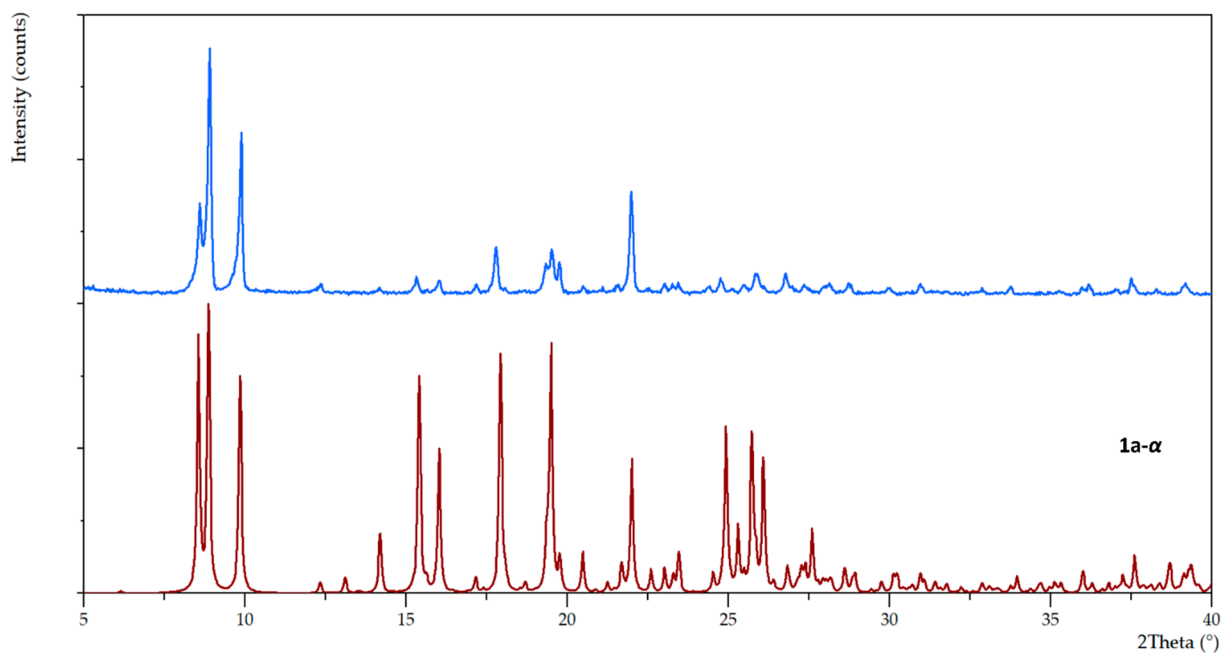


**Figure S5.** Experimental PXRD pattern (blue) of the products of synthesis no. 5 from Table S1 compared with calculated PXRD patterns from the crystal structure of **1a- $\alpha$**  (red).

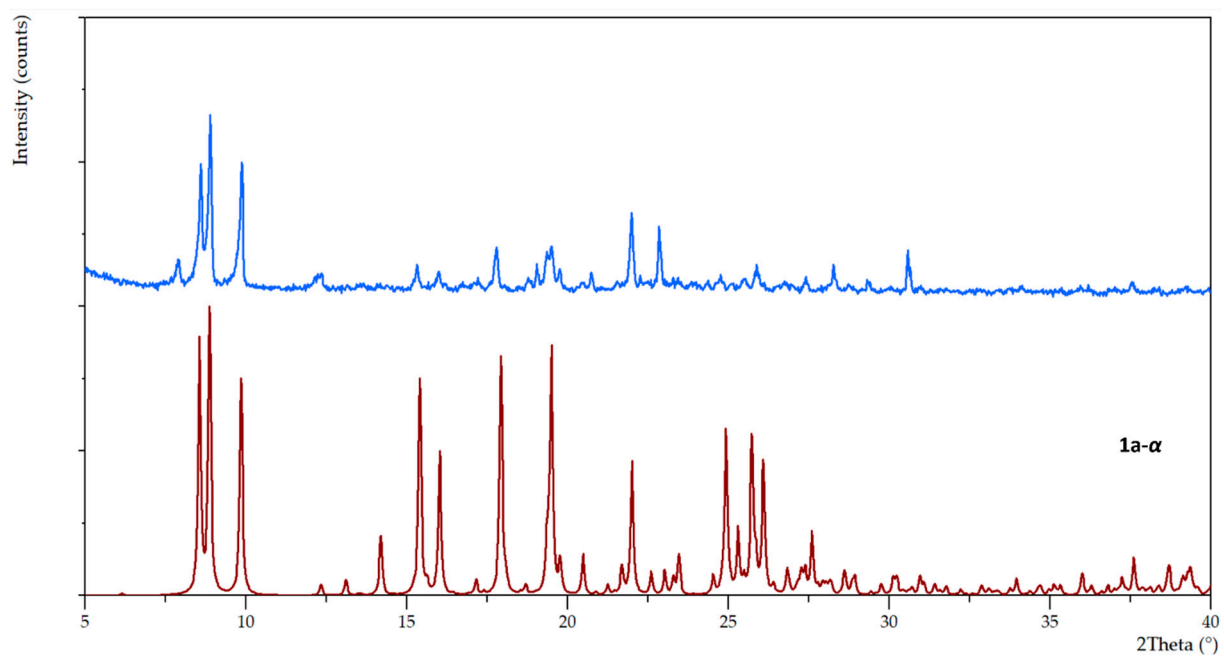


**Figure S6.** Experimental PXRD pattern (blue) of the products of synthesis no. 6 from Table S1 compared with calculated PXRD patterns from the crystal structure of **1a- $\alpha$**  (red).

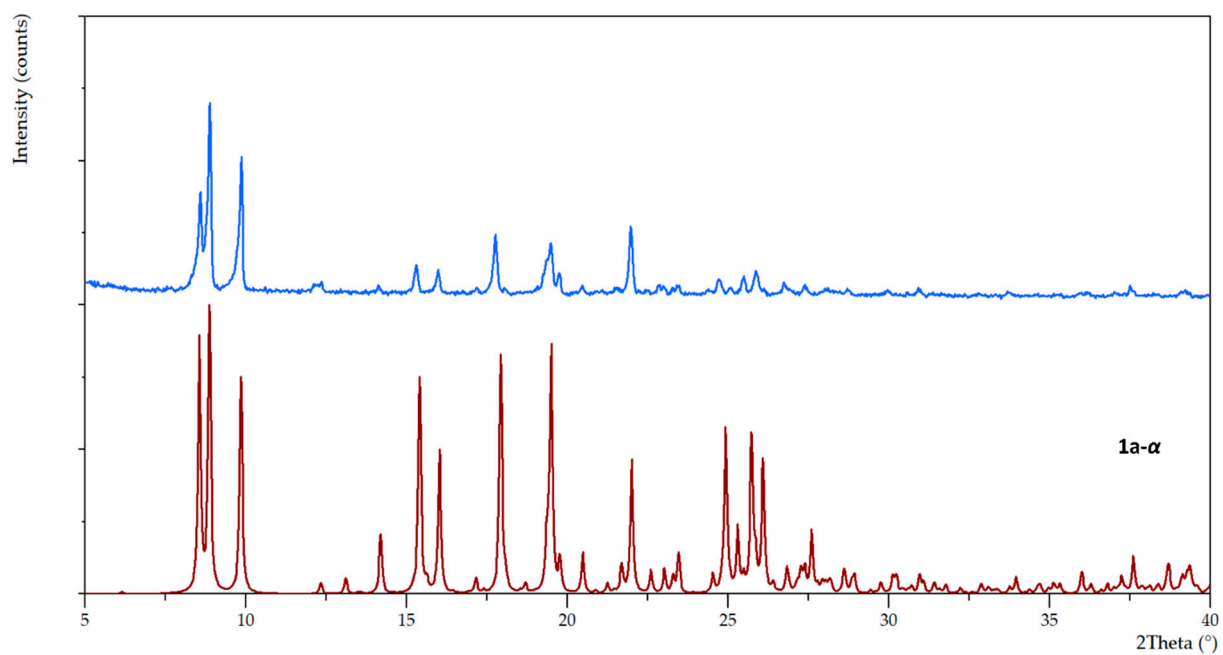


**Figure S7.** Experimental PXRD pattern (blue) of the products of synthesis no. 7 from Table S1 compared with calculated PXRD patterns from the crystal structure of **1a- $\alpha$**  (red).

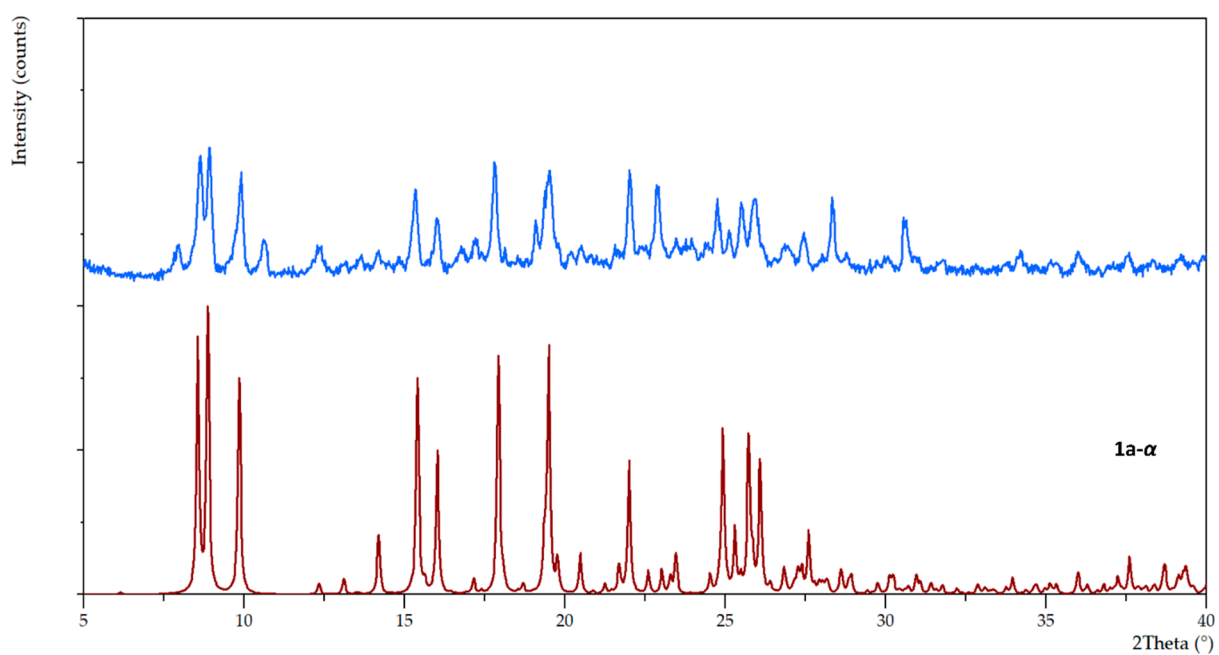


**Figure S8.** Experimental PXRD pattern (blue) of the products of synthesis no. 8 from Table S2 compared with calculated PXRD patterns from the crystal structure of **1a- $\alpha$**  (red).

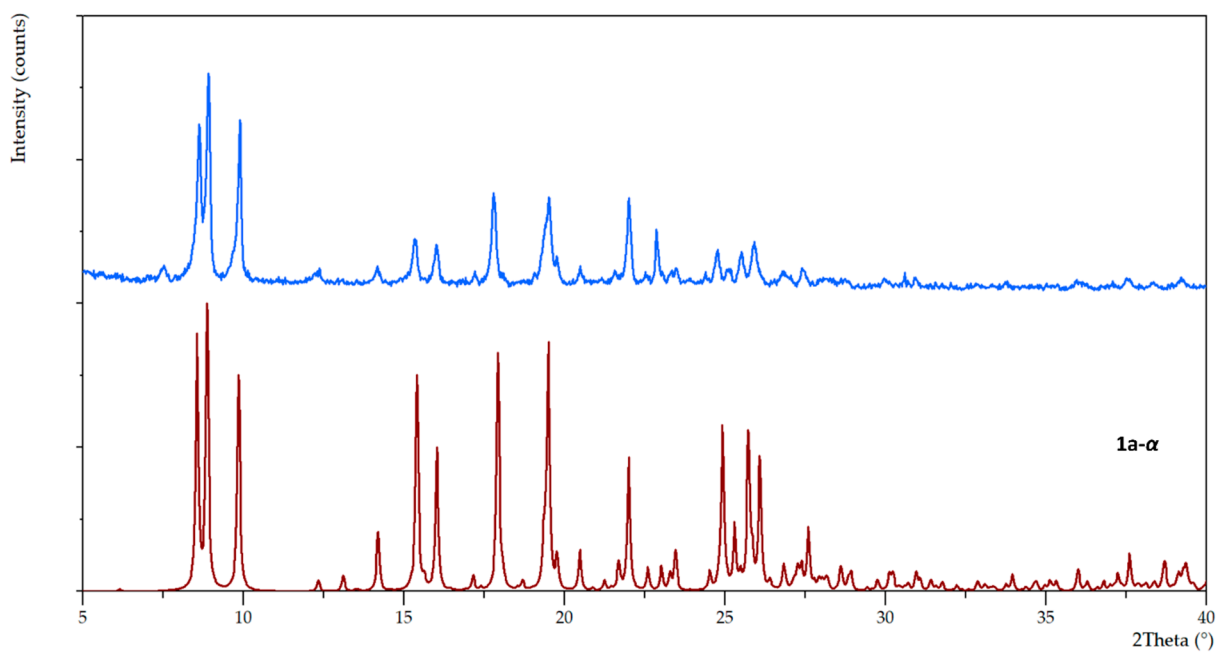


**Figure S9.** Experimental PXRD pattern (blue) of the products of synthesis no. 9 from Table S2 compared with calculated PXRD patterns from the crystal structure of **1a-α** (red).

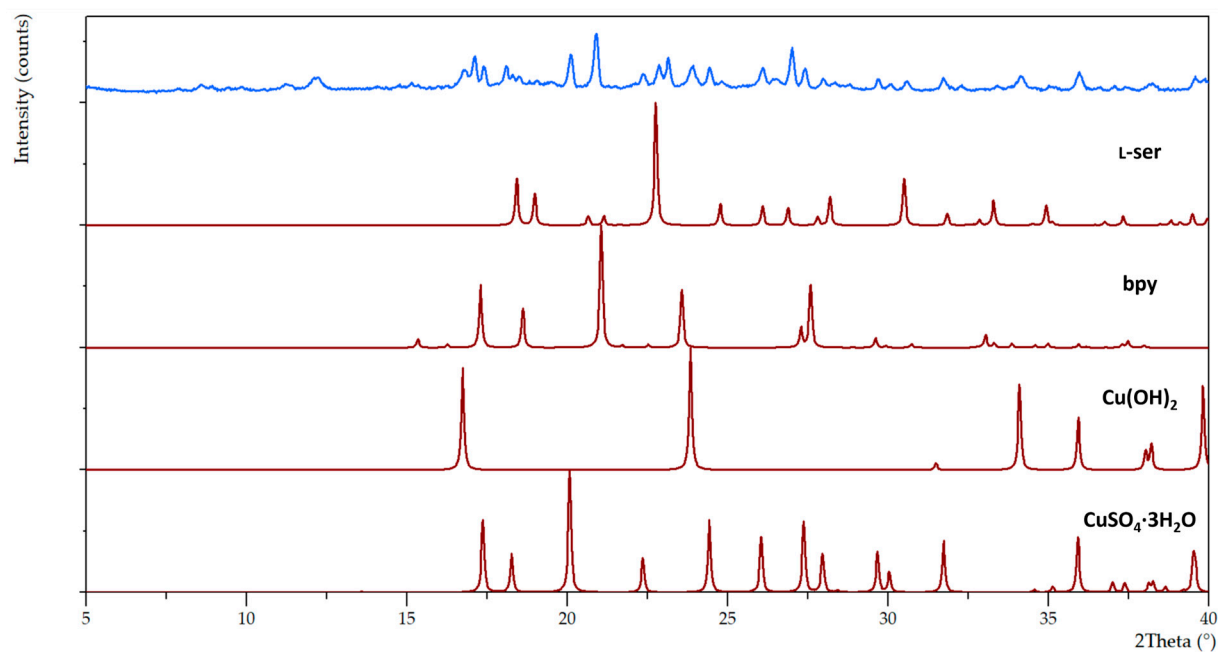


**Figure S10.** Experimental PXRD pattern (blue) of the products of synthesis no. 10 from Table S2 compared with calculated PXRD patterns from the crystal structures of reactants (red).

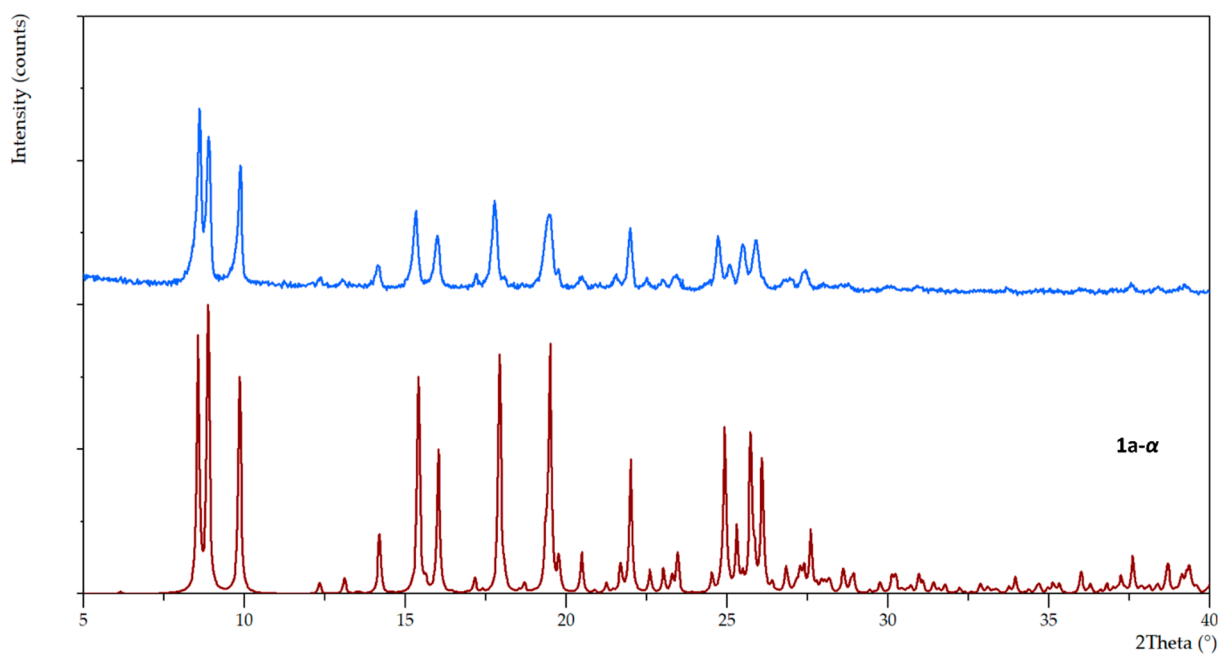


**Figure S11.** Experimental PXR D pattern (blue) of the products of synthesis no. 11 from Table S2 compared with calculated PXR D patterns from the crystal structure of **1a- $\alpha$**  (red).

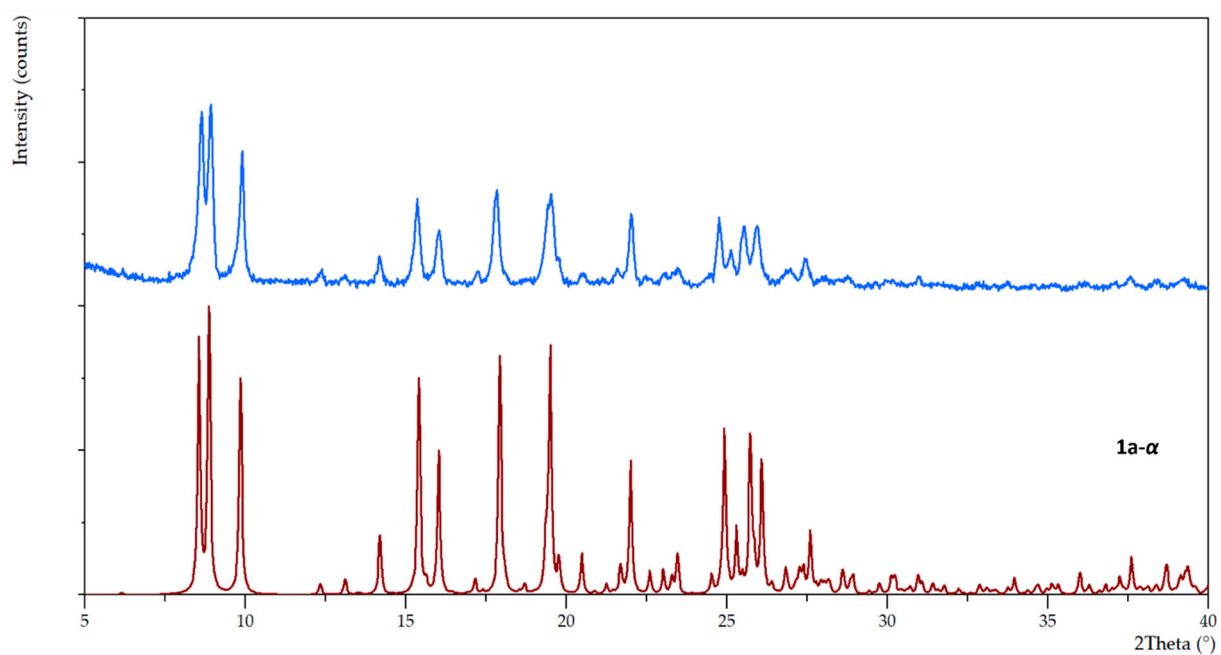


**Figure S12.** Experimental PXR D pattern (blue) of the products of synthesis no. 12 from Table S2 compared with calculated PXR D patterns from the crystal structure of **1a- $\alpha$**  (red).

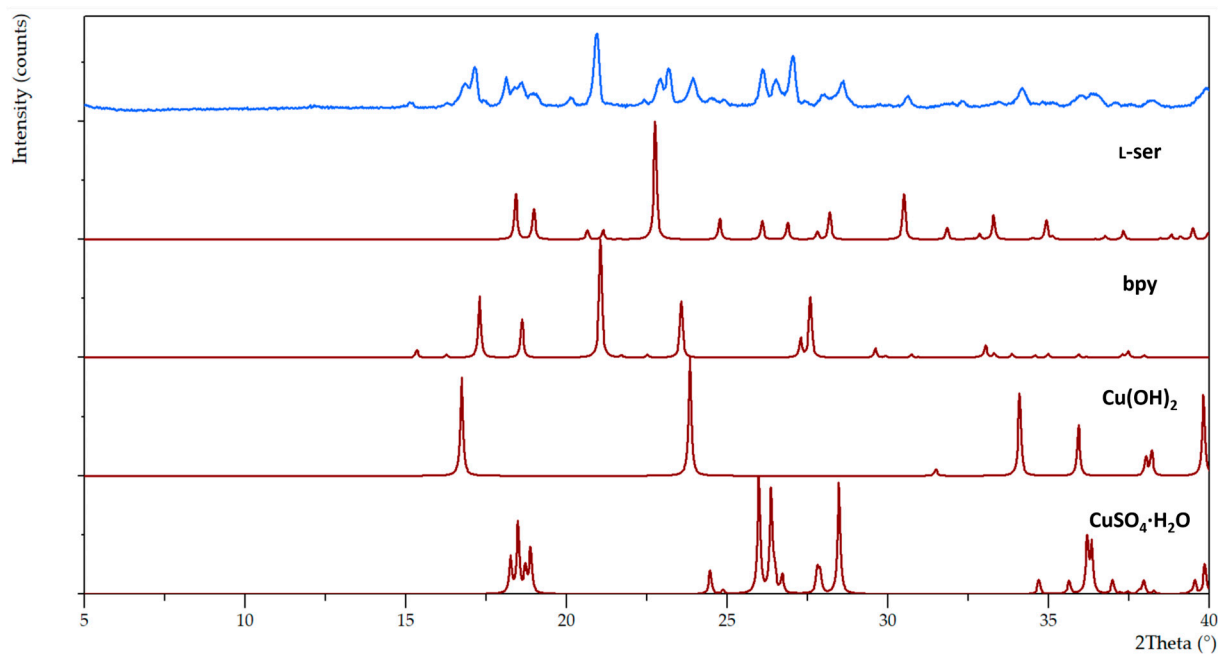


**Figure S13.** Experimental PXRD pattern (blue) of the products of synthesis no. 13 from Table S2 compared with calculated PXRD patterns from the crystal structures of reactants (red).

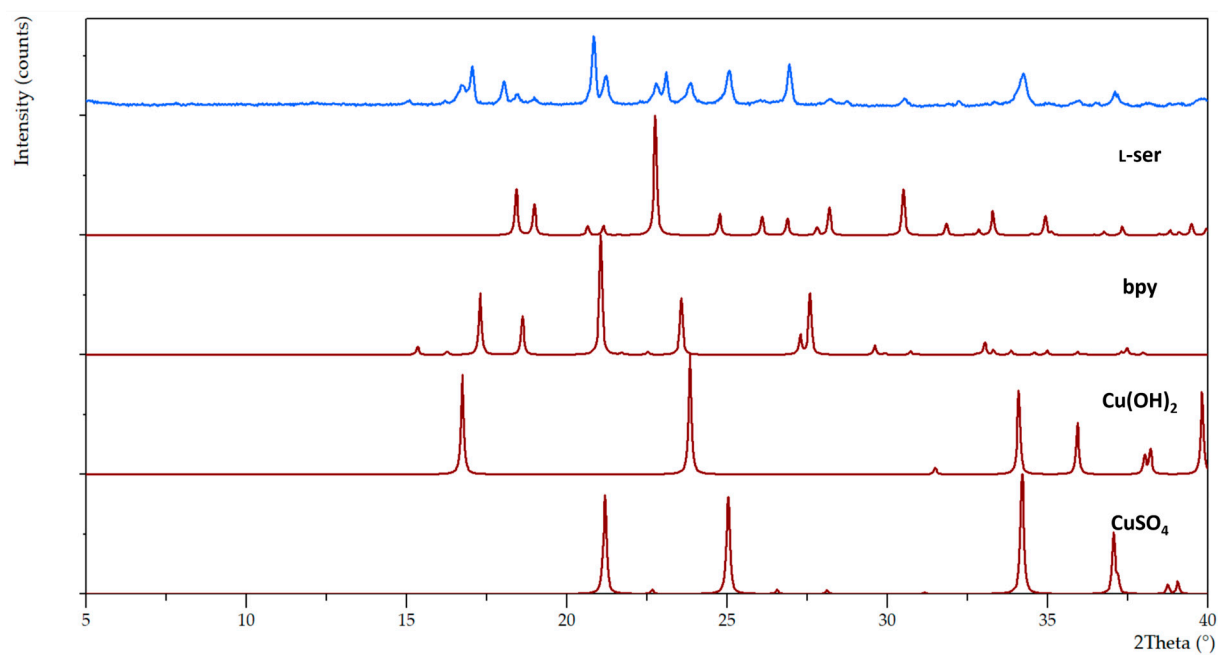


**Figure S14.** Experimental PXRD pattern (blue) of the products of synthesis no. 14 from Table S3 compared with calculated PXRD patterns from the crystal structures of reactants (red).

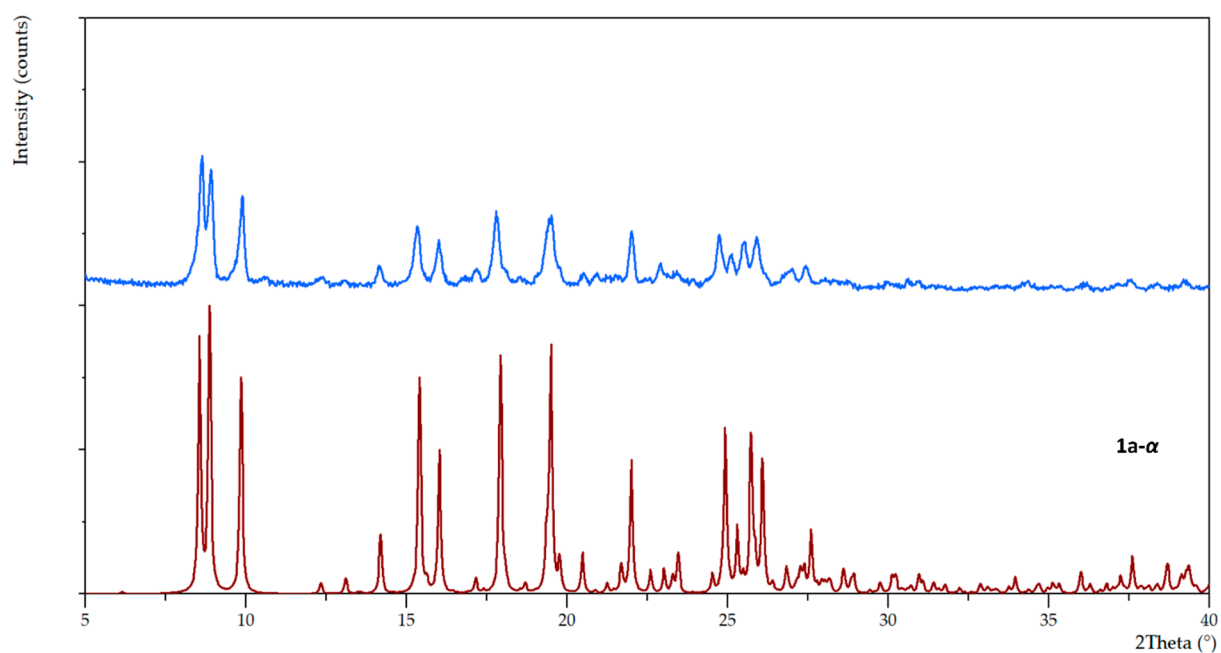


**Figure S15.** Experimental PXR D pattern (blue) of the products of synthesis no. 15 from Table S3 compared with calculated PXR D patterns from the crystal structure of **1a- $\alpha$**  (red).

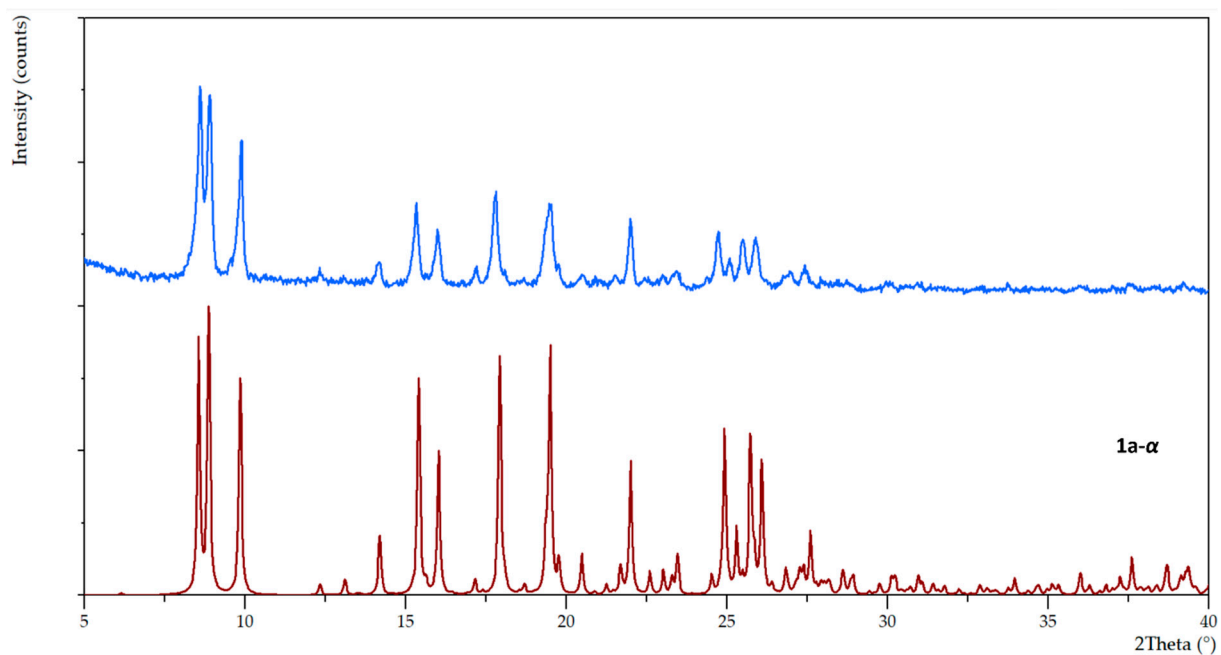


**Figure S16.** Experimental PXR D pattern (blue) of the products of synthesis no. 16 from Table S3 compared with calculated PXR D patterns from the crystal structure of **1a- $\alpha$**  (red).

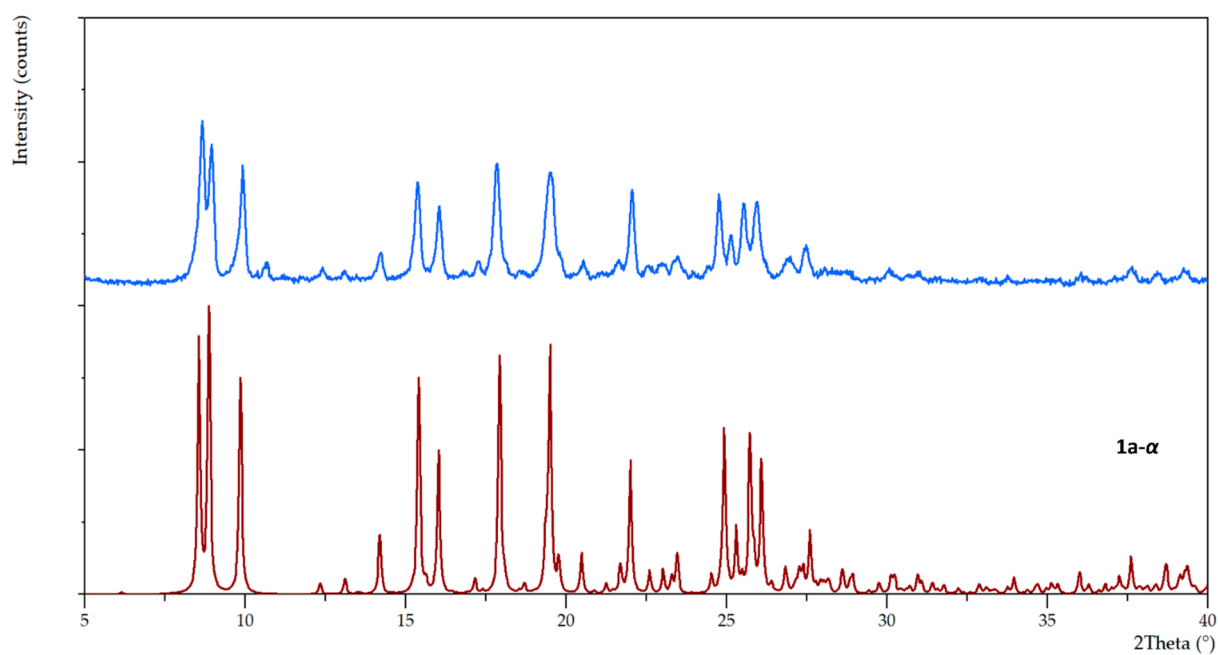


**Figure S17.** Experimental PXR D pattern (blue) of the products of synthesis no. 17 from Table S3 compared with calculated PXR D patterns from the crystal structure of **1a-α** (red).

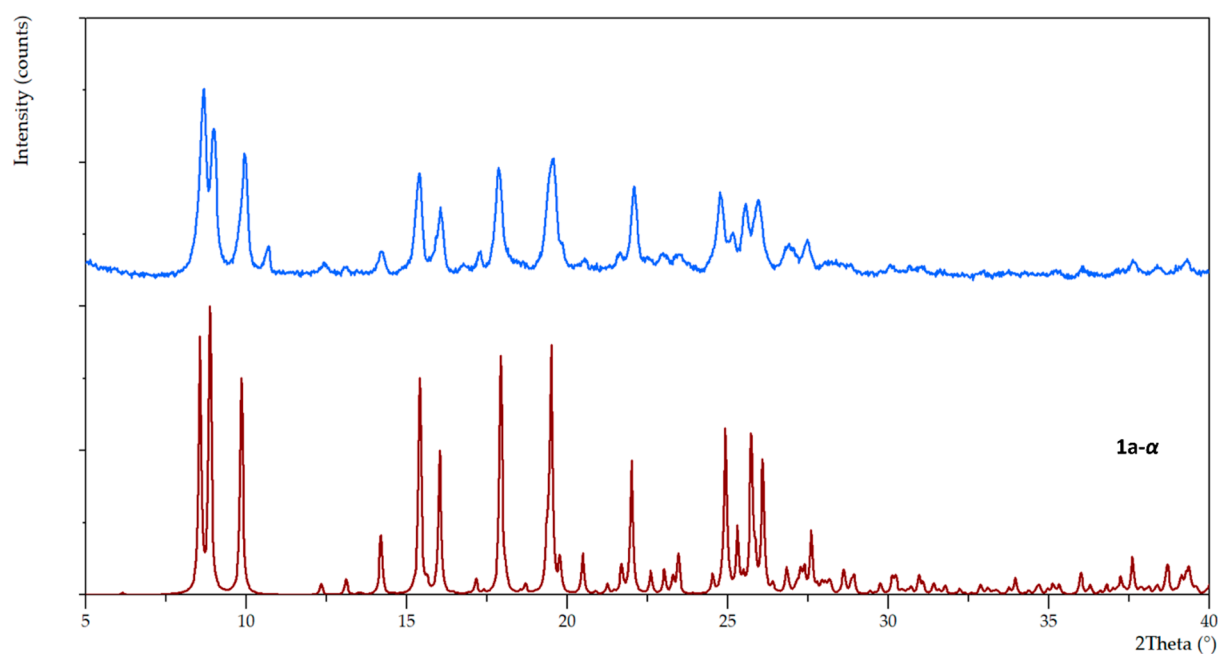


**Figure S18.** Experimental PXR D pattern (blue) of the products of synthesis no. 18 from Table S3 compared with calculated PXR D patterns from the crystal structure of **1a-α** (red).

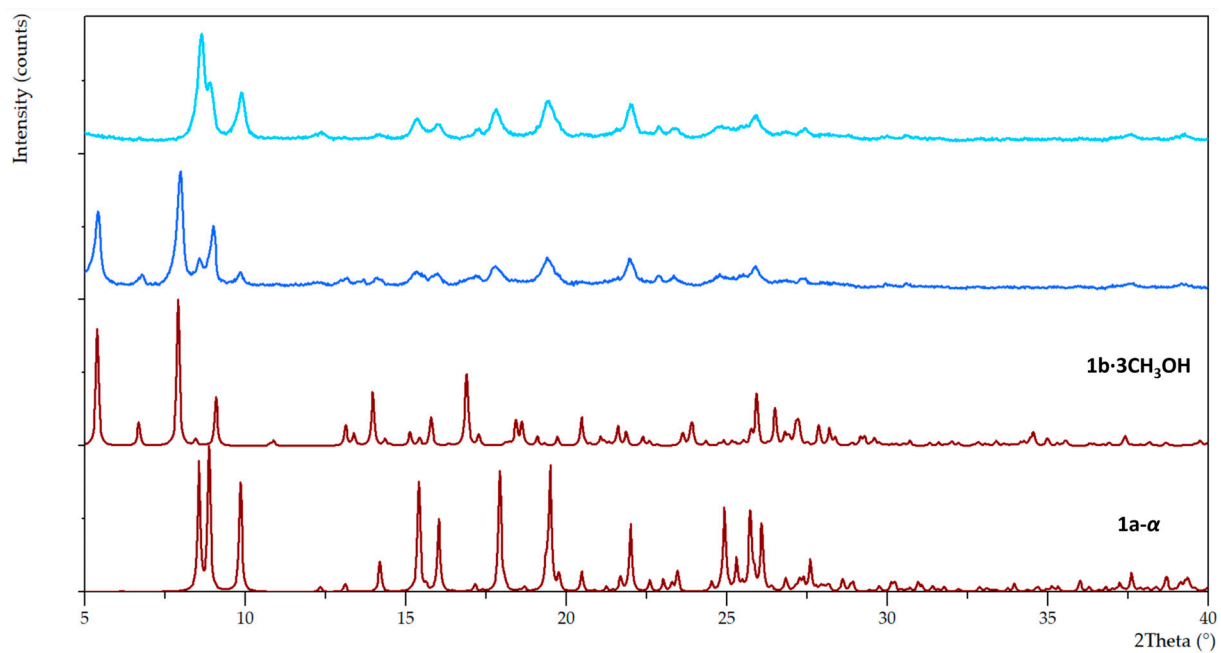


**Figure S19.** Experimental PXRD pattern of the products of synthesis no. 19 from Table S3 measured immediately upon opening the jar (blue) and after 2 min of standing in the air (light blue) compared with calculated PXRD patterns from the crystal structures of **1a- $\alpha$**  and **1b·3CH<sub>3</sub>OH** (red).

## 2. Transformations $1\mathbf{a}\cdot 6\mathbf{H}_2\mathbf{O} \rightleftharpoons 1\mathbf{a}\cdot \alpha$

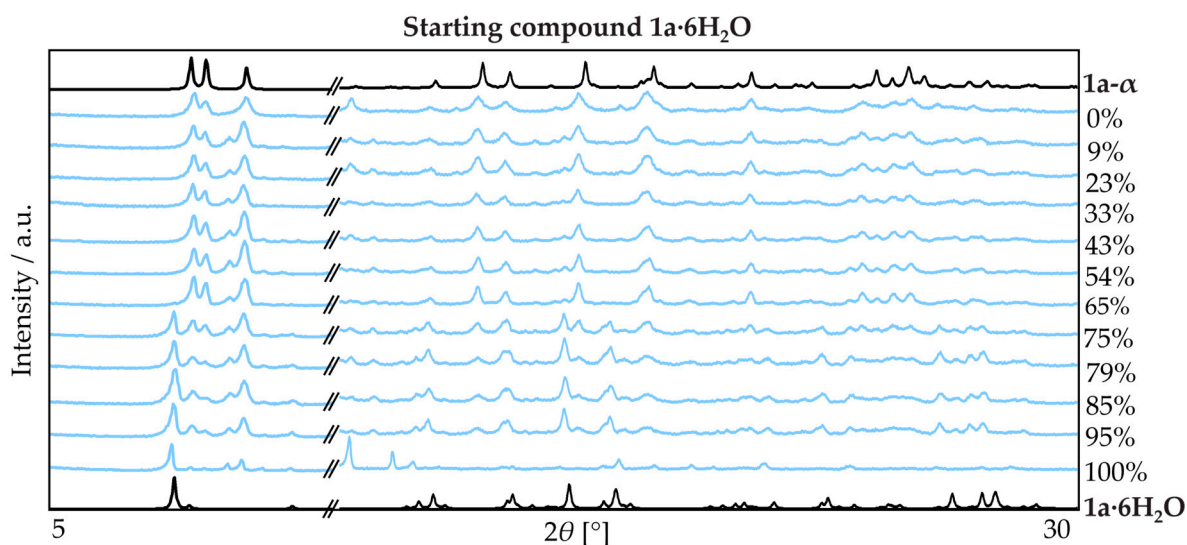


**Figure S20.** Experimental PXRD patterns of  $1\mathbf{a}\cdot 6\mathbf{H}_2\mathbf{O}$  after aging 4 weeks (blue) in a humidity- and temperature-controlled chamber compared with calculated PXRD patterns from the crystal structures of  $1\mathbf{a}\cdot \alpha$  and  $1\mathbf{a}\cdot 6\mathbf{H}_2\mathbf{O}$  (black).

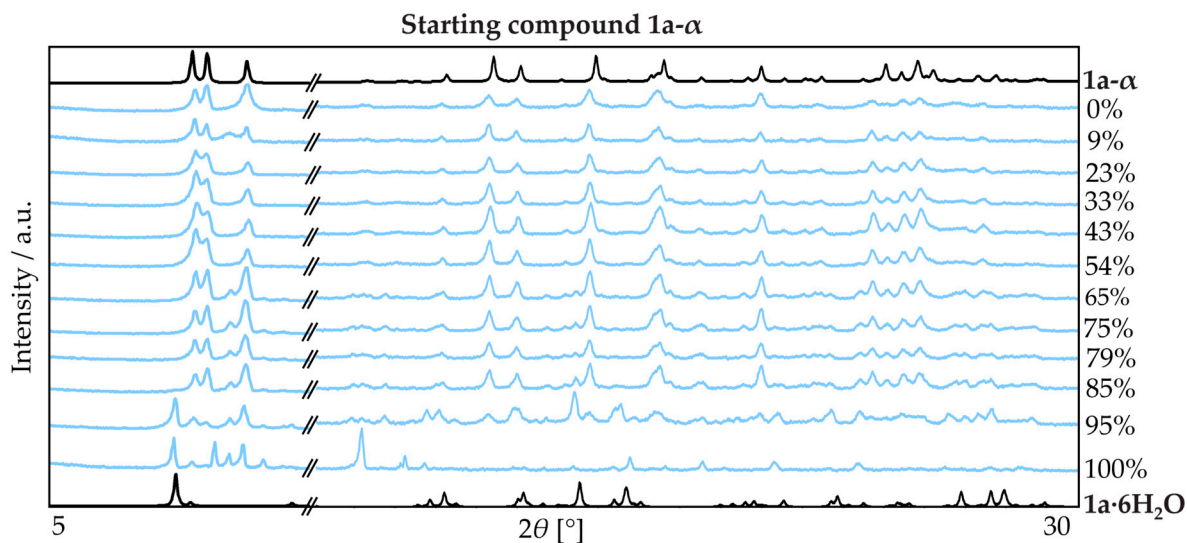


**Figure S21.** Experimental PXRD patterns of  $1\mathbf{a}\cdot \alpha$  after aging 4 weeks (blue) in a humidity- and temperature-controlled chamber compared with calculated PXRD patterns from the crystal structures of  $1\mathbf{a}\cdot \alpha$  and  $1\mathbf{a}\cdot 6\mathbf{H}_2\mathbf{O}$  (black).

### 3. Thermogravimetric analysis and infrared spectroscopy

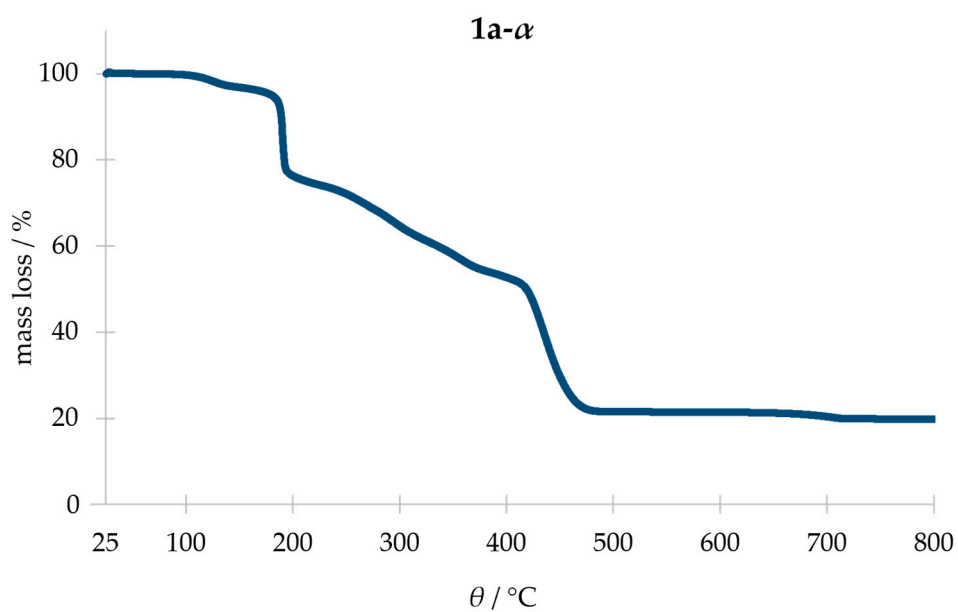


**Figure S22.** TGA curve of **1a- $\alpha$** .

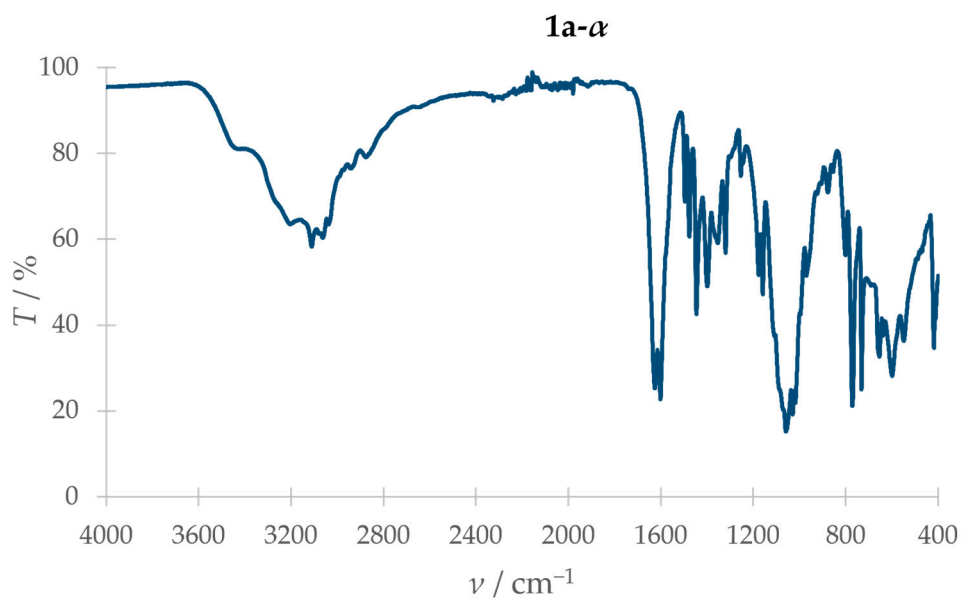


**Figure S23.** IR(ATR) spectrum of **1a- $\alpha$** .

#### 4. Crystal structures

**Table S4.** Crystallographic data for compounds **1a- $\alpha$** , **1a- $\beta$** , **1a·6H<sub>2</sub>O**, and **1b·3CH<sub>3</sub>OH**.

	<b>1a-<math>\alpha</math></b>	<b>1a-<math>\beta</math></b>	<b>1a·6H<sub>2</sub>O</b>	<b>1b·3CH<sub>3</sub>OH</b>
Formula	C <sub>26</sub> H <sub>32</sub> Cu <sub>2</sub> N <sub>6</sub> O <sub>12</sub> S	C <sub>26</sub> H <sub>32</sub> Cu <sub>2</sub> N <sub>6</sub> O <sub>12</sub> S	C <sub>26</sub> H <sub>44</sub> Cu <sub>2</sub> N <sub>6</sub> O <sub>18</sub> S	C <sub>31</sub> H <sub>48</sub> Cu <sub>2</sub> N <sub>6</sub> O <sub>15</sub> S
Formula weight [g mol <sup>-1</sup> ]	779.71	779.71	887.81	903.89
$\lambda$ [Å]	sync, 0.70000	1.54184	sync, 0.70000	sync, 0.70000
Crystal system	monoclinic	monoclinic	monoclinic	orthorhombic
Space group	<i>P</i> 2 <sub>1</sub>	<i>P</i> 2 <sub>1</sub>	<i>P</i> 2 <sub>1</sub>	<i>P</i> 2 <sub>1</sub> 2 <sub>1</sub> 2 <sub>1</sub>
<i>a</i> [Å]	7.1389(1)	10.0790(3)	6.7125(1)	6.8675(1)
<i>b</i> [Å]	20.7625(4)	20.9260(5)	20.8435(2)	20.9159(2)
<i>c</i> [Å]	20.0048(4)	14.5656(3)	13.1341(1)	26.4444(3)
$\alpha$ [°]	90	90	90	90
$\beta$ [°]	95.348(2)	107.209(3)	103.455(1)	90
$\gamma$ [°]	90	90	90	90
<i>V</i> [Å <sup>3</sup> ]	2952.23(9)	2934.55(14)	1787.18(4)	3798.47(8)
<i>Z</i>	4	4	2	4
<i>T</i> [K]	100	100	100	100
$\rho$ [g cm <sup>-3</sup> ]	1.754	1.765	1.650	1.581
$\mu$ [mm <sup>-1</sup> ]	1.455	3.129	1.221	1.203
$\theta$ range [°]	2.0, 25.9	3.2, 68.2	1.6, 30.0	1.8, 30.0
Obs. reflections ( <i>I</i> > 2 $\sigma$ ( <i>I</i> ))	10731	10378	9957	11324
Number of parameters	881	876	526	514
<i>R</i> <sub>1</sub> (observed reflections) <sup>1</sup>	0.0673	0.0620	0.0335	0.0496
<i>wR</i> <sub>2</sub> (all data) <sup>2</sup>	0.1637	0.1561	0.0937	0.1349
<i>S</i> <sup>3</sup>	1.06	1.06	1.04	1.04
min/max residual electron density [Å <sup>-3</sup> ]	-0.72, 1.25	-0.77, 0.91	-0.55, 0.82	-0.63, 0.87
CCDC no.	2393622	2393624	2393621	2393623

**Table S5.** Distances ( $\text{\AA}$ ) within the polyhedra of copper coordination spheres in the crystal structures of **1a- $\alpha$** , **1a- $\beta$** , **1a·6H<sub>2</sub>O**, and **1b·3CH<sub>3</sub>OH**.

<b>Bond lengths [<math>\text{\AA}</math>]</b>				
	<b>1a-<math>\alpha</math></b>	<b>1a-<math>\beta</math></b>	<b>1a·6H<sub>2</sub>O</b>	<b>1b·3CH<sub>3</sub>OH</b>
Cu1-O11	1.936(9)	1.949(6)	1.932(3)	1.932(3)
Cu1-O13	2.249(8)	2.298(6)	2.252(3)	-
Cu1-O1M	-	-	-	2.234(3)
Cu1-N1	1.989(10)	1.986(8)	1.994(2)	2.005(3)
Cu1-N11	1.982(9)	1.988(7)	2.005(2)	2.004(3)
Cu1-N110	1.994(10)	2.004(7)	1.992(2)	2.004(3)
Cu2-O21	1.940(8)	1.947(6)	1.945(2)	1.923(3)
Cu2-O23	2.205(8)	2.302(6)	2.253(3)	-
Cu2-O2M	-	-	-	2.347(4)
Cu2-N2	2.011(10)	1.992(7)	1.994(2)	1.974(3)
Cu2-N21	2.002(8)	1.980(7)	1.999(3)	1.993(4)
Cu2-N210	2.012(10)	2.005(7)	1.993(3)	1.993(3)
Cu3-O31	1.951(8)	1.941(6)	-	-
Cu3-O33	2.225(8)	2.221(7)	-	-
Cu3-N3	1.995(9)	1.991(8)	-	-
Cu3-N31	2.000(10)	1.999(7)	-	-
Cu3-N310	2.009(10)	2.021(8)	-	-
Cu4-O41	1.943(8)	1.955(7)	-	-
Cu4-O43	2.216(9)	2.228(6)	-	-
Cu4-N4	2.002(10)	2.002(8)	-	-
Cu4-N41	2.009(10)	2.008(8)	-	-
Cu4-N410	2.010(10)	2.039(8)	-	-

**Table S6.** Selected hydrogen bonds in **1a- $\alpha$** , **1a- $\beta$** , **1a·6H<sub>2</sub>O**, and **1b·3CH<sub>3</sub>OH**.

Compound	D-H...A	$d(\text{D-H}\cdots\text{A}) / \text{\AA}$	$\angle(\text{D-H}\cdots\text{A}) / ^\circ$
<b>1a-<math>\alpha</math></b>	O13-H13A...O31	2.952(13)	133(12)
	O23-H23B...O41	3.131(11)	145(9)
	O1G-H1G...O24S	2.56(2)	131
	O4G2-H4G2...O11S	2.730(16)	164
	N4-H4B...O3G	3.133(12)	152
<b>1a-<math>\beta</math></b>	O13-H13A...O12S	2.711(9)	159(9)
	O23-H23A...O41 <sup>1</sup>	3.069(9)	153(11)
	O23-H23B...O21S	3.102(10)	125(9)
	O33-H33A...O11S	2.654(11)	166(13)
	O43-H43A...O24S	2.674(10)	173(9)
	O1G-H1G1...O21S	2.828(15)	172
	O2G-H2G...O11S	2.584(11)	126
	O3G-H3G...O23S	2.650(10)	153
	N1-H1B...O4G	3.403(11)	168
	N2-H2A...O3G	2.931(10)	176
	N3-H3B...O2G	3.229(10)	156
<b>1a·6H<sub>2</sub>O</b>	O1W-H1WB...O12	2.665(4)	171(4)
	O13-H13A...O3W	2.697(4)	174(3)
	O23-H23A...O1W	2.771(3)	172(3) <sup>1</sup>
	O23-H23B...O13S <sup>2</sup>	2.729(3)	171(4)
	O2W-H2WA...O11S	2.882(4)	165(6)
	O1G-H1G...O11S	2.844(4)	155
	O2G-H2G...O14S <sup>2</sup>	2.736(4)	164
	N1-H1C...O2G	3.201(4)	157
<b>1b·3CH<sub>3</sub>OH</b>	O1M-H1M...O12 <sup>3</sup>	2.634(4)	171(5)
	O2M-H2M...O2S <sup>2</sup>	2.614(5)	171(6)
	O3M-H3M...O1S	2.759(6)	157(9)
	O1G-H1G...O4S	2.799(4)	169
	O2G-H2G...O3S <sup>4</sup>	2.712(4)	168
	N1-H1B...O2G	3.037(4)	160

<sup>1</sup>-1+x,y,-1+z; <sup>2</sup>-x,-1/2+y,-z; <sup>3</sup>1+x,y,z; <sup>4</sup>1-x,1/2+y,1/2-z

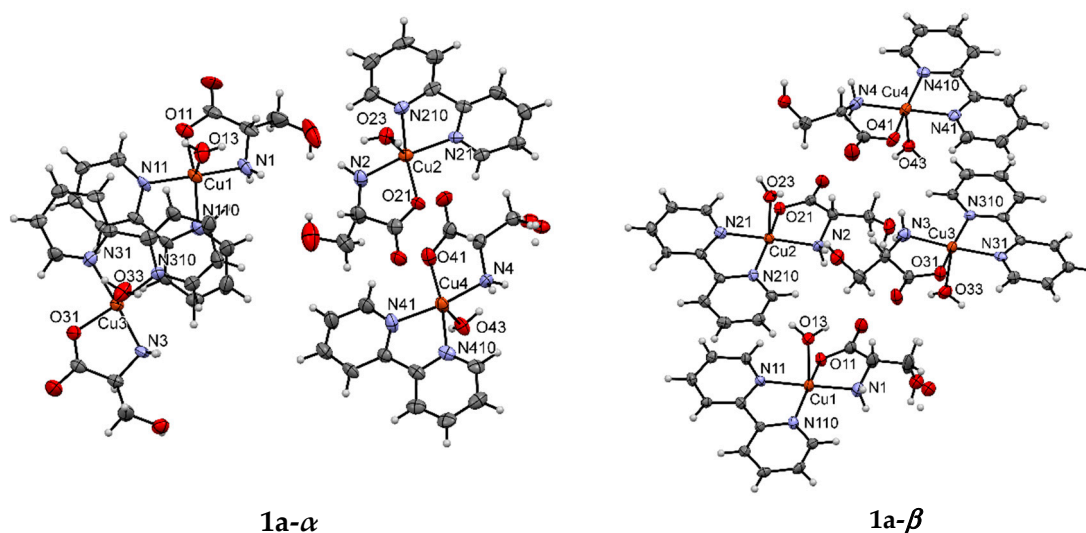


**Figure S24.** ORTEP plot of the asymmetric unit of **1a- $\alpha$**  and **1a- $\beta$** , with the atom labelling scheme in the copper coordination sphere. Crystallization water molecules and sulfate anion were omitted for clarity. Displacement ellipsoids were calculated at the 50% probability level.

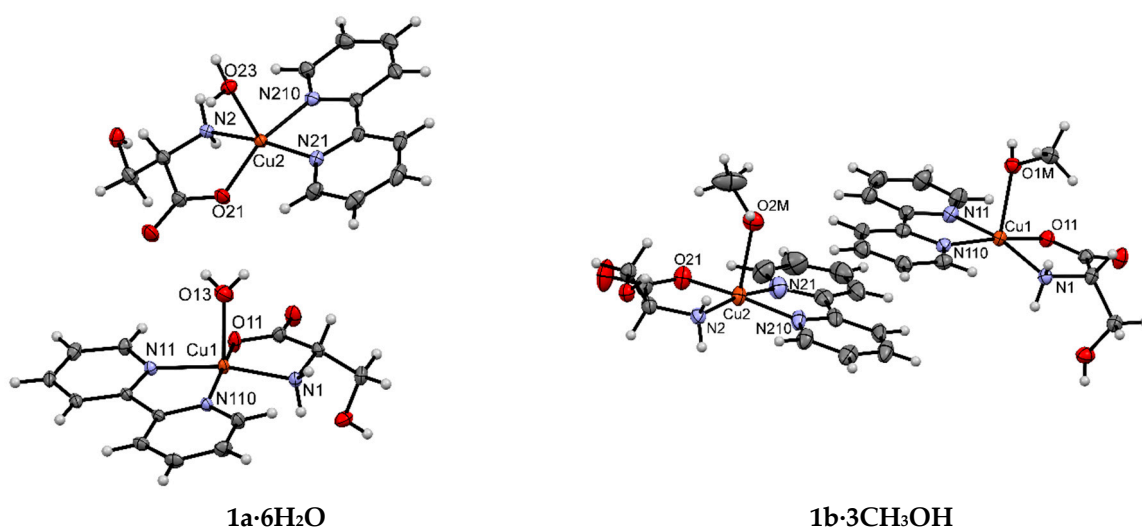


**Figure S25.** ORTEP plot of the asymmetric unit of **1a·6H<sub>2</sub>O** and **1b·3CH<sub>3</sub>OH** with the atom labelling scheme in the copper coordination sphere. Crystallization water/methanol molecules and sulfate anion were omitted for clarity. Displacement ellipsoids were calculated at the 50% probability level.

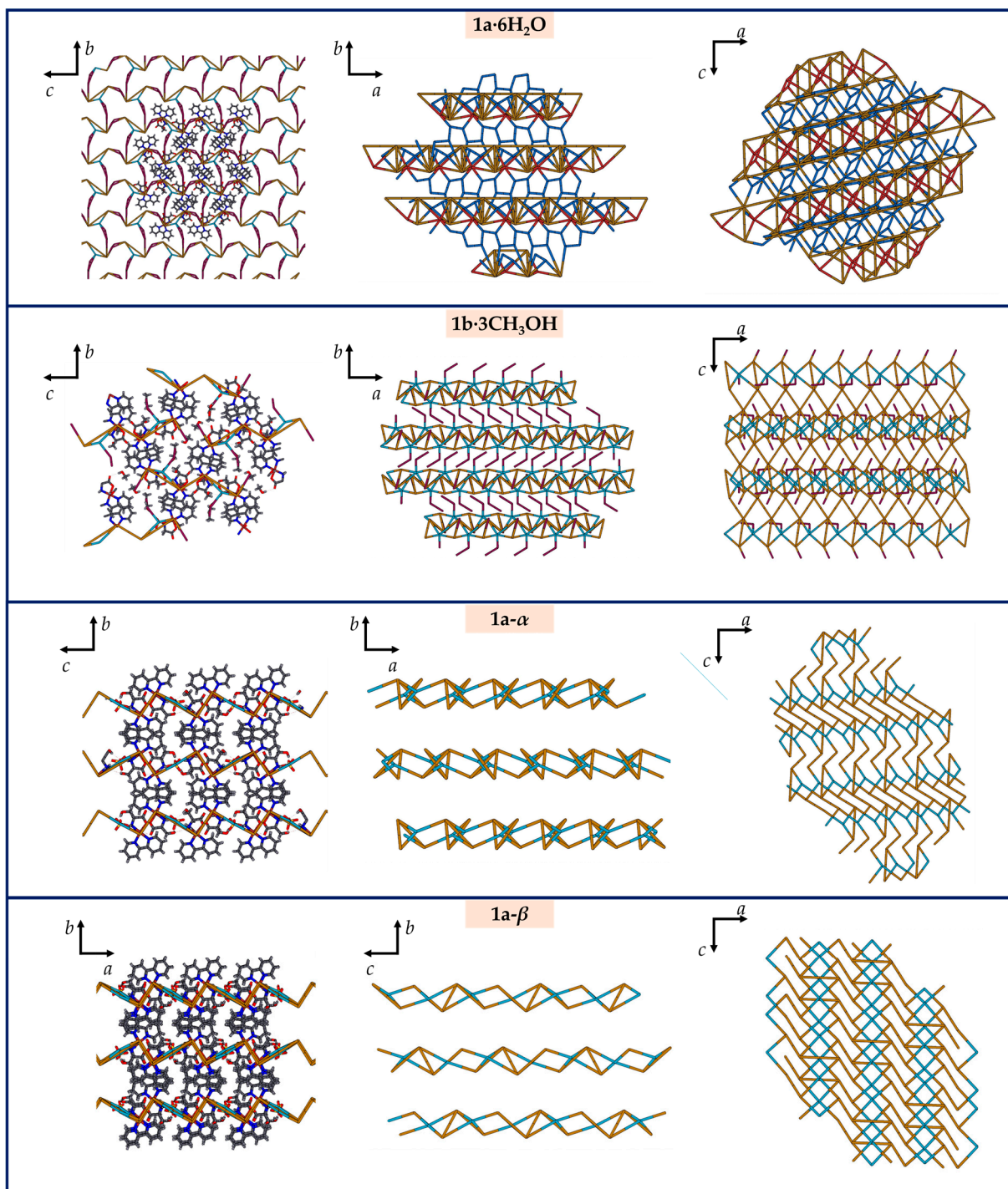


**Figure S26.** Simplified hydrogen bond frameworks. Brown lines represent hydrogen bonds formed by complex cations  $[\text{Cu}(\text{L-ser})(\text{L})(\text{bpy})]^+$  ( $\text{L} = \text{H}_2\text{O}$  or  $\text{CH}_3\text{OH}$ ); light blue lines, hydrogen bonds formed by sulfate ions; dark blue lines, hydrogen bonds formed by crystallization water molecules in  $\mathbf{1a}\cdot\mathbf{6H}_2\mathbf{O}$ ; and purple lines, hydrogen bonds formed by crystallization methanol molecules in  $\mathbf{1b}\cdot\mathbf{3CH}_3\mathbf{OH}$ . Atoms are shown in the pictures on the left, while the pictures in the middle and on the right, they are omitted for clarity.

## 5. Proliferation assays

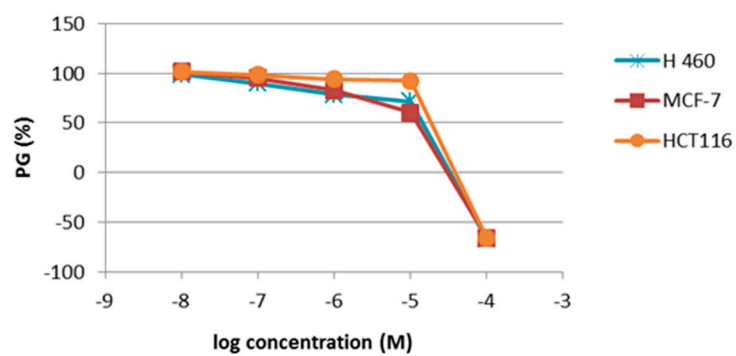


**Figure S27.** Concentration–response profiles for **1a- $\alpha$**  tested in vitro on HCT116, MCF-7, and H 460 cell lines.